Community structures in allelopathic interaction networks: An ecoevolutionary approach

S. A. Carvalho [1,2,*] and M. L. Martins [1,3,4,†]

[1] *Departamento de Física, Universidade Federal de Viçosa, 36570-900, Viçosa, Minas Gerais, Brazil*

[2] *IFMG, Campus Formiga, 35577-010, Formiga, Minas Gerais, Brazil*

[3] *National Institute of Science and technology for Complex Systems, Centro Brasileiro de Pesquisas Físicas, Rua Xavier Sigaud 150, 22290-180, Rio de Janeiro, Brazil*

[4] *Ibitipoca Institute of Physics (IbitiPhys), 36140-000–Conceição do Ibitipoca–MG, Brazil*

(Received 6 November 2019; revised 23 July 2020; accepted 22 September 2020; published 8 October 2020)

Evidence is mounting that the race of living organisms for adaptation to the chemicals synthesized by their neighbors may drive community structures. Here, an ecoevolutionary model for community assembly through resource competition, toxin-mediated interactions (allelopathy), and evolutionary branching is investigated. We found that stable communities with increasing biodiversity can emerge at weak allelopathic suppression, but strong chemical warfare drastically impairs diversity. For successive invasion events, the allelopathic interaction networks exhibit, respectively, Gaussian and Weibull degree distributions at weak and strong allelopathy. For the branching process dynamics, degrees scale as power laws truncated by stretched exponentials in both regimes. In addition, allelochemical interactions tend to be arranged in modules with low clustering coefficients and disassortative behavior to ensure community stability. So, in a homogeneous environment, species-rich communities can be assembled only at the context of a weak biochemical warfare between organisms, and even under this regime species interact with only a few others.

DOI: 10.1103/PhysRevE.102.042305

I. INTRODUCTION

Conventional explanations of biodiversity postulate that it is passively shaped by niche differentiation, density-dependent predation pressure, habitat heterogeneity, or fluctuations in the resources required by the biological communities. Furthermore, stabilizing mechanisms relying on negative intraspecific interactions, stronger than interspecific interactions, are essential for species coexistence [1] since they cause species to limit themselves more than other organisms. Without stabilizing mechanisms, the inhibitory effects of competition on inferior competitors will ultimately lead to their extinction. Classically, such stabilizing interactions have been thought to result from resource partitioning: Competing species can coexist provided they are most limited by different resources and consume the resources they are most limited by at a higher rate than do other species [2].

However, the conventional view that biodiversity is ruled by resource competition is challenged by the extraordinary species richness observed within microorganism communities in seemingly uniform environments. Indeed, only a highly structured habitat could sustain large diversities, but not even such astronomical species numbers. Again, we are looking at the famous paradox of the plankton [3]. Moreover, experiments performed with plants have neither shown intraspecific unequivocally exceeding interspecific competition [4] nor competing plants coexisting through resource partitioning [5]. Also, abiotic supply rates seems to be relatively high and stable over time, whereas the resident species neither reduce resource densities nor interfere greatly with resource access [6].

In contrast, interference competitions mediated by the production of toxic chemical compounds—antibiotic, phytotoxins, lactate, etc.—are ubiquitous in biological communities, from microorganisms, such as bacteria [6], yeasts [7], and other fungi [8] to cancer cells [9,10] and plant invasions [11]. So, in addition to other nontrophic interactions (e.g., the rise of mycorrhizal networks in plant communities [12], mutualism at weak direct competition [13], and facilitation [14], the biochemical warfare between living organisms may drive species coexistence and community composition. Nonetheless, the alternative explanation for the emergence of biological communities driven by competing interactions between their species is challenging—mainly, if such interactions involve inhhibitions or suppressions mediated by toxins released in the environment, i.e., allelopathy. Intuitively, multiple toxic environments are the least expected to sustain great biological diversity. Indeed, some invasive plants release secondary metabolites (allelochemicals) to disrupt the native communities they invade [15,16]. Therefore, community and invasion ecology are naturally interconnected because both the persistence of a species in a community or its invasion success abroad its native habitat primarily depends on its ability to increase from low density [17–19].

In this paper, our goal is to discuss how community structures of populations enforced to adapt and survive the direct allelochemical suppression of each other is affected by the evolutionary history of the interaction. Specifically, we

*sylvestre.carvalho@gmail.com

†mmartins@ufv.br

extend previously proposed models for the allelopathic warfare between two species [20–22] by integrating ecological and evolutionary processes. In the model, the genetic diversity is generated by mutations that induce changes in the allelochemical traits of the evolving species and selection is driven by ecological interactions, namely, intra- and interspecific resource competition and allelopathic suppression. These interactions determine how species evolve and enhance or diminish the diversity of communities. A minor part of the results studied in this paper was previously reported in Ref. [22]. We decided to include such results, but extended and more thoroughly discussed.

II. ECOEVOLUTIONARY MODEL FOR ALLELOPATHIC COMMUNITIES

To model the community dynamics, a set S of $l \in \mathbb{N}$ biological species with populations given by $\mathbf{N} = (N_1, N_2, \ldots, N_l)$ is considered. The interactions among these species occurs only via intra- and interspecific resource competition and allelopathic suppression. Thus, every species in S synthesizes and releases toxic secondary chemical compounds (microcins, fitotoxins, etc.) that enhance the mortality of other species. The strengths of such interactions depends on the toxin concentration $\mathbf{B} = (B_1, B_2, \ldots, B_l)$ and vary in time because $\mathbf{B}$ depends on the abundance of the species. Furthermore, the community assembly proceeds from an initial subset $S_0 \subseteq S$ by randomly adding new species through mutations fixed in a fraction of resident species' offspring.

A. Ecological dynamics

The temporal evolution of the biological community in a homogeneous environment is described by the coupled ordinary differential equations:

$$\frac{dN_i}{dt} = r_i \left(1 - \sum_{j=1}^{l} \nu_{ij} N_j\right) N_i - \sum_{j \neq i}^{l} \mu_{ij} \Phi_{ij}^{(k)} N_i,$$
$$\frac{dB_i}{dt} = \beta_i N_i - \delta_i B_i - \sum_{j \neq i}^{l} \gamma_{ji} N_j B_i. \quad (1)$$

Here, N_i stands for the population density of the species i that produces the allelochemical concentration B_i, respectively. Also, r_i, β_i and δ_i, $i = 1, 2, \ldots$, respectively, are the reproduction, toxin release, and natural degradation rates associated to the competing species. A classical interspecific competition for the environmental resources is assumed. The parameters ν_{ij} are the competition coefficients that measure the extent to which each species presses upon the resources used by the others. The term $-\sum_{j \neq i} \mu_{ij} \Phi_{ij}^{(k)}(y_j)$ represents species decreases induced by the allelochemicals released by their allelopathic suppressors, in which μ_{ij} is the mortality rate of the species i induced by the toxin released by its competitor j. Finally, the quantity $y_j = \gamma_{ji} N_i B_j$ represents the overall consumption of the toxin j by the species i, $i \neq j$, with per capta absorption rate γ_{ij}. These quantities depend on the toxin's levels in a linear way. Different Holling types I, II, and III functional responses were assumed,

$$\Phi_{ij}^{(k)} = \begin{cases} \frac{B_j}{B_0} & (k = 1) \\ \frac{B_j}{c_i + B_j} & (k = 2) \\ \frac{B_j^2}{c_i + B_j^2} & (k = 3), \end{cases} \quad (2)$$

where the parameter $B_0 \equiv 1$ is the slope of the linear response used to make it dimensionless and c_i controls the toxin's efficiencies in poisoning their competing species. All these response functions assume null thresholds for toxin effects, but those with $k > 1$ impose saturation to the allelopathic suppression. Also, all the response functions involve the total toxin concentration.

Equations (1) and (2) for two species were extensively investigated through analytical and numerical methods in Refs. [20–22]. In the present paper, up to $l = 100$ competing species were considered and the interacting parameters $\nu_{i,j}$, $\gamma_{j,i}$, and $\mu_{i,j}$ define networks in which the species are the nodes. These parameters can be expressed as $\nu_{i,j} = \nu_{i,j}\, \varepsilon_{i,j}$, $\gamma_{j,i} = \gamma_{j,i}\, \zeta_{j,i}$, and $\mu_{i,j} = \mu_{i,j}\, \zeta_{i,j}$, in which $\varepsilon_{i,j} = 1$ ($\zeta_{i,j} = 1$) if species i competes with (poisons) species j, but $\varepsilon_{i,j} = 0$ ($\zeta_{i,j} = 0$) if i does not compete (poisons) j. Every $\varepsilon_{i,j}$, $\zeta_{i,j} = 1$ is a link connecting two species. The set of values $\varepsilon_{i,j}$ and $\zeta_{i,j}$ define two matrices ε and ζ which characterize the competition and allelochemical interaction networks, respectively. These matrices are examples of the adjacency matrix, central in network theory [23–25]. The diagonal elements of ε are $\varepsilon_{i,i} = 1$ and represent intraspecific competition, with all $\nu_{i,i} = 1$ by definition. In turn, we set all $\zeta_{i,i} = 0$ to avoid self-allelopathic suppression.

Under competition and allelopathy, the system dynamics—Eq. (1)—reaches a stationary state ($\mathbf{N}^*$, $\mathbf{B}^*$) determined by the species initially present and their ecological interactions. Even at weak interspecific competition (the coexistence regime), some populations are eventually extinct and the community diversity (species richness) decreases.

B. Evolutionary dynamics

The interplay between evolutionary processes and ecological interactions among species drives the origin and maintenance of biological communities [26]. In our mathematical model, ecology and evolution are integrated by assuming that mutations in one of the competing species generate a new one. Such mutations, occurring after the community reaches a stationary state, is the source of genetic diversity and disturbs the system dynamics. Indeed, the newly introduced species, as well as the old ones in the community, must survive and evolve in response to novel conditions. Ultimately, the ecological dynamics reaches another stationary state comprised by distinct populations and interaction networks. Two mechanisms for species introduction were tested.

1. Sequential invasion events

In a stationary community currently comprised by n species, an alien species is introduced and a new node, $n + 1$, representing it is added to the ecological interaction network. Since we assume that this alien species competes for resources with all the n species already present in the community, their

matrix elements in the competition interaction network are $\varepsilon_{n+1,i} = \varepsilon_{i,n+1} = 1$ for $i = 1, \ldots, n$. In turn, concerning allelochemical suppression, we assume that the alien species affects k_{n+1}^{out} of the old ones and is affected by k_{n+1}^{in} of them. So, k_{n+1}^{out} elements $\zeta_{n+1,i}$ in the row $n+1$ of the enlarged adjacency matrix ζ are fixed in 1 and the remaining in 0. To do this, an integer i is randomly chosen in the interval $[1, n]$, and we set $\zeta_{n+1,i} = 1$, with a probability $p = 1 - n^{\text{out}}/n$, or $\zeta_{n+1,i} = 0$, with a probability $1 - p = n^{\text{out}}/n$. Then, a distinct i is randomly selected and the protocol repeated until k_{n+1}^{out} elements in the $(n+1)$th row of ζ are set to 1. The value $n^{\text{out}} \in [1, n]$ defines the probability p and, again, is an integer random number chosen with equal change. On average, n^{out} determines the fraction of species in the community which do not interact with the alien species. Analogously, k_{n+1}^{in} elements $\zeta_{i,n+1}$ in the column $n+1$ of the enlarged adjacency matrix are fixed in 1 and the remaining in 0. The same protocol is used to determine the k_{n+1}^{in} nodes i that suppress the node $n+1$ (i.e., $\zeta_{i,n+1} = 1$). But now the probability used is $p = 1 - n^{\text{in}}/n$. Finally, the initial toxin concentration of the alien species is $B_{n+1} = 0$ and its population density is $N_{n+1} = 0.01N_i^*$, with N_i^* corresponding to the stationary population density of one species chosen at random between the n current members of the community. Regarding the initial community structure, the sequential invasion event (SIE) evolutionary dynamics starts from a single species.

2. Branching process

The new species $n+1$ introduced in the network descends from one of the n species present at the community stationary state. The ancestor species i is randomly chosen and only their allelochemical traits are mutated in its descendant species $n+1$. Specifically, all the k_i^{in} input and k_i^{out} output connections of the ancestor node i are inherited by the new node $n+1$, except one of them. With equal chance, either a randomly chosen input $\zeta_{j,i}$ or output $\zeta_{i,j}$ of node i will be activated ($\zeta_{j,n+1} = 1$) in node $n+1$ if inactive ($\zeta_{j,i} = 0$) in i, or vice versa. Since its is supposed here that the resource competition traits are not changed by mutations, $\varepsilon_{i,j} = \varepsilon_{n+1,j}$ and $\varepsilon_{j,i} = \varepsilon_{j,n+1}$ for $j = 1, \ldots, n$. Again, the initial toxin concentration of the new species is $B_{n+1} = 0$ and its population density is $N_{n+1} = 0.01N_i^*$. Finally, concerning the initial community structure, the branching process (BP) evolutionary dynamics starts from a network with $n_0 < l$ nodes. Different starting graphs for the BP dynamics are shown in Fig. 1.

C. Numerical integration

The previously described ecoevolutionary processes were investigated through numerical integration using the fourth-order Runge-Kutta method. Distinct distributions for the values of the competition and allelochemical parameters ϵ_{ij} and ζ_{ij} were employed. Also, 200 independent evolutionary histories were generated for the SIE and BP dynamics, in the latter case for each initial graph shown in Fig. 1. From the numerical integrations, the adjacency matrix at the successive stationary states for each evolutionary history were obtained. Then, the community structures (interaction network topologies) and species richness were determined for both SIE and BP dynamics.

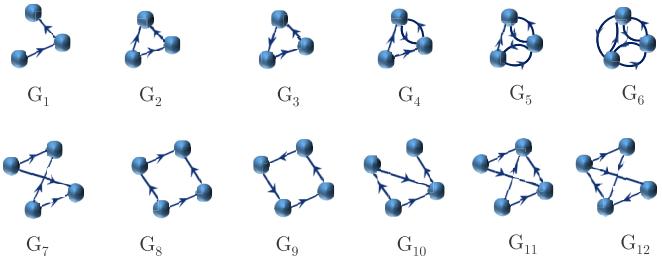

FIG. 1. Allelopathic networks used as starting structures for the BP dynamics. The species interactions are indicated by arrows. In numerical integrations, the population densities N_i (0) = 0.7 and toxin concentrations B_i (0) = 0 were fixed.

III. RESULTS

The SIE and BP dynamics were analyzed for three distinct scenarios considering functional responses 2. In the first one, called a homogeneous SIE, all the original and introduced species have equal competition and allelopathic traits: $r_i = 1\ \forall i$, $\nu_{ij} = 0.1$ and $\epsilon_{ij} = 1$, $\forall i, j$ and $\gamma_{ij} = 0.1$, $\forall i, j$, $c_i = 0.1$, $\beta_i = 0.1$, and $\delta_i = 0.2$, with weak ($\mu_{ij} = 0.1$) or strong ($\mu_{ij} = 0.5$) alellopathic suppression $\forall i, j$. In the second scenario, called heterogeneous competition, the allelochemical traits are equal, as before, but the mortality effect is weak ($\mu_{ij} = 0.1$) and competition coefficients ν_{ij} are disordered, i.e., randomly drawn from a uniform distribution on the interval (0,1]. Thus, the species can have different competition but the same allelochemical capabilities. Finally, in the third scenario, called completely heterogeneous, it is supposed that both competition and allelochemical traits are disordered and independently drawn from uniform distributions on the interval (0,1]. Only the toxins' degradation and uptaken rates, $\delta_i = 0.2$ and $\gamma_{ji} = 0.1$, are assumed the same for all species. For BP dynamics, the scenarios are the same of SIE except in completely homogeneous scenarios was tested only for weak allelopathic suppression ($\mu_{ij} = 0.1$) $\forall i, j$. Results concerning the absorption effect in the response functions 2 are reported in the Supplemental Material [27].

In Fig. 2, the average diversity as a function of the number n_{SIE} and n_{BP} of, respectively, SIE and BP events are shown. The diversity is defined as the number of surviving species at the new community stationary state reached after an SIE or BP event. For the SIE dynamics, communities exhibiting large diversities can be assembled at weak allelopathy ($\mu = 0.1$). This is the rule for all response functions tested. Moreover, the diversity decreases as the response to toxins increases, as should be expected. Indeed, except for small ($x < 0.11$) or large ($x > 0.89$) toxin concentrations, the inequalities $\Phi^{(1)}(x) < \Phi^{(3)}(x) < \Phi^{(2)}(x)$ are satisfied in our simulations. In contrast, strong allelopathic suppressions drastically reduce community diversity [see Supplemental Fig. 1(a)]. In addition, community diversity is reduced when competition ($\nu_{ij} \in (0, 1]$) or competition and allelopathy are heterogeneous (all parameters are drawn from random distributions, except $r_i = 1$, $\delta_i = 0.2$, and $\gamma_{ij} = 0.1\ \forall i, j$). The introduction of heterogeneity in competition coefficients has stronger effects as shown in Fig. 2(b). In comparison with Fig. 2(a), a drastic decrease in diversity is observed even

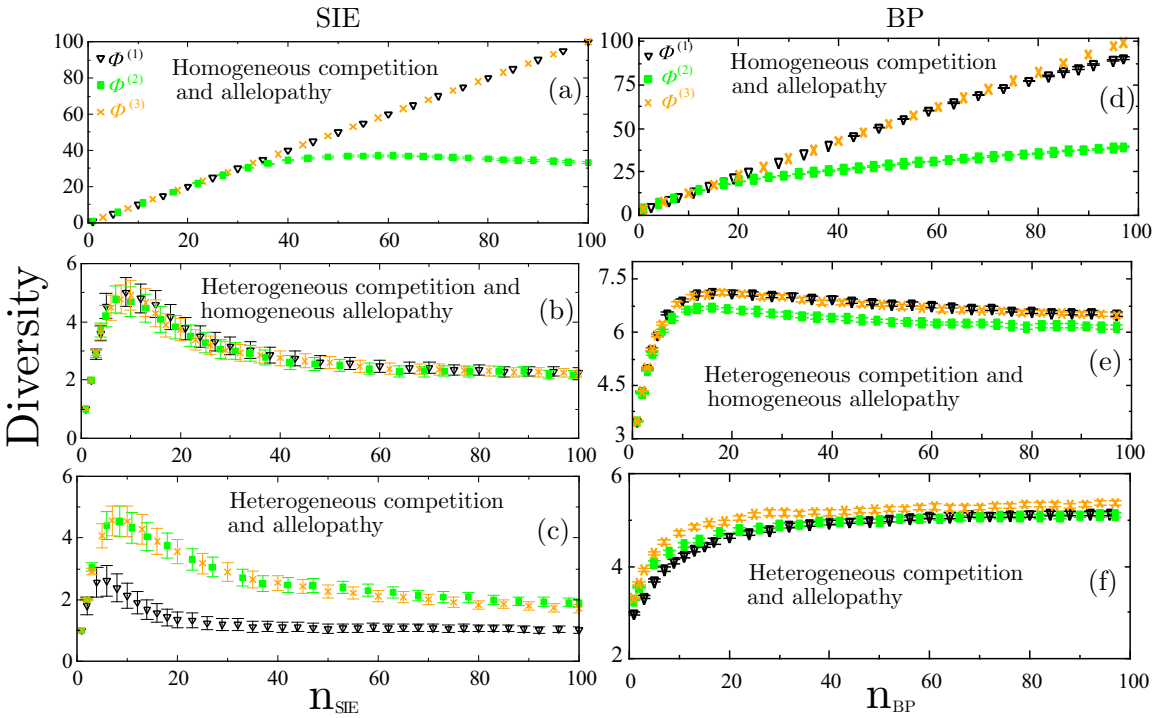

FIG. 2. Average diversity for 200 independent ecoevolutionary histories as function of the number n_{SIE} and n_{BP} observed after successive invasion events SIE (a)–(c) and branching process BP (d)–(f). In the SIE dynamics, the community always starts from a single species, whereas in BP dynamics the initial communities are the graphs shown in Fig. 1. The upper, middle, and bottom plots refer, respectively, to homogeneous ($r_i = 1$, $\nu_{ij} = \mu_{ij} = \gamma_{ij} = 0.1$, $c_i = \beta_i = 0.1$, and $\delta_i = 0.2$ $\forall i, j$) competition and allelopathic suppression, heterogeneous competition ($\nu_{ij} \in (0, 1]$, randomly drawn), and completely heterogeneous (both competition ν_{ij} and allelopathic μ_{ij}, c_i, and β_i parameters randomly chosen in (0,1]) scenarios. Diversities for typical individual realizations, shown in Supplemental Fig. 3, evidence the presence of small noises leading to very smooth average curves.

under weak allelopathy $\mu = 0.1$ and for all response functions. The same qualitative behavior is observed in BP dynamics (see Figs. 2(d)–2(f), where the middle and bottom plots evidence that heterogeneous competition and allelochemical traits strongly decrease community diversity in comparison to homogeneous traits (upper plot). Disorder (heterogeneities) in the allelochemical traits further reinforces extinctions in the network. Finally, we believe that the monotonous increase of diversity observed for weak homogeneous competition and allelopathy with functional responses $\Phi^{(1,3)}$ will eventually stop at larger numbers of invasion or speciation events. After that, the diversity will decrease and behaves similarly to the regimes of strong allelopathy or heterogeneous competition (which exhibit saturation). Hence, after an eventual saturation, the statistical properties for these weak interactions recovery those of heterogeneous scenarios.

The degree distributions $P(k)$ for allelochemical interaction networks generated by the SIE (a,b) and BP (c-e) dynamics are shown in Fig. 3. Normal (Gaussian) and Weibull distributions were observed for in- and out-degree distributions $P(k_{in})$ and $P(k_{out})$ (data not shown) depending on the mortality μ induced by allelopathy in SIE. For weak allelopathic suppression, $P(k_{in})$ is a Normal distribution [see Fig. 3(a)]. In contrast, at strong allelopathic suppression, $P(k_{in})$ is Weibull distributed. The apparent anisotropies observed in the insets for $\Phi^{(1,2,3)}$ are very weak, as supported by skewness $S \sim 0$ and kurtosis $K \sim 3$. The ratio $\langle k^2\rangle/\langle k\rangle$ is obtained for either weak or strong allelopathic suppression μ, indicating that the SIE allelochemical networks are homogeneous [23]. The in- and out-degree distributions, $P(k_{in})$ and $P(k_{out})$, for the allelochemical interaction networks generated by the BP dynamics are fitted by power-laws truncated by stretched exponentials $P(k) \sim k^{-\alpha} \exp(-\eta\, k^{\lambda})$ (Weibull-like distributions). The ratio $\langle k^2\rangle/\langle k\rangle \sim \langle k\rangle$ is observed only for both competition and allelopathy homogeneous and weak ($\nu < 1$ and $\mu = 0.1$), indicating the homogeneous nature of such networks. In contrast, $\langle k^2\rangle/\langle k\rangle \gg \langle k\rangle$ was found for the remaining cases: (i) weak homogeneous competition ($\nu < 1$) and strong homogeneous allelopathy ($\mu = 0.5$), (ii) weak heterogeneous competition ($\nu_{ij} \in (0, 1]$ randomly chosen) and weak homogeneous allelopathy ($\mu = 0.1$), and (iii) heterogeneous competition and allelopathy (ν_{ij}, μ_{ij}, c_i and $\beta_i \in (0, 1]$ chosen at random). In these regimes, the emergence of heterogeneous networks is expected.

In Fig. 4, the average betweenness centrality $\langle x_i\rangle$ is plotted for every node i present at the stationary allelochemical network after $l = 100$ SIE [Figs. 4(a) and 4(b)] and BP events Figs. 4(c)–4(e). In SIE, $\langle x_i\rangle$ decreases dramatically as the strength of allelopathic suppression increases. Also, the stronger the responses to toxins ($\Phi^{(2)}$ for $\mu = 0.1$ and $\Phi^{(2,3)}$ for $\mu = 0.5$), the smaller is $\langle x_i\rangle$. Furthermore, the average centrality is almost constant at weak allelopathic suppression, indicating a homogeneous connectivity pattern for every node and the absence of hubs, bridges joining distinct modules,

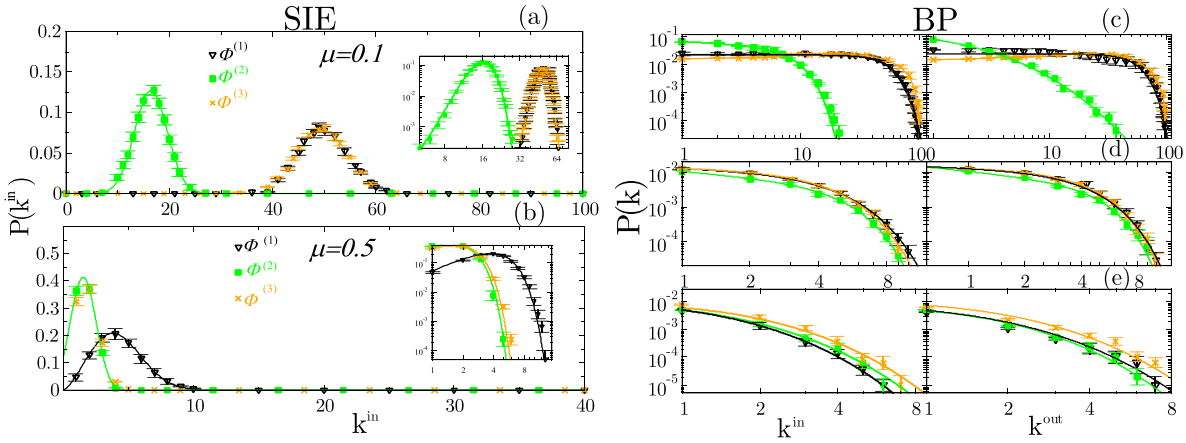

FIG. 3. Degree distributions $P(k)$ for SIE (a), (b) and BP (c), (e) allelochemical interaction networks in which the competition and allelochemical traits are the same for all species. In SIE dynamics, the plots refer to homogeneous scenarios ($r_i = 1$, $\nu_{ij} = \gamma_{ij} = 0.1$, $c_i = \beta_i = 0.1$, and $\delta_i = 0.2$ $\forall i, j$) in weak ($\mu_{ij} = 0.1$) and strong ($\mu_{ij} = 0.5$) allelopathic suppression regimes. Insets: Log-log plots of the in-degree distributions. For the BP dynamics, the in- and out-degree distribution functions in directed allelochemical networks are shown. The upper, middle, and bottom plots refer, respectively, to homogeneous, heterogeneous competition, and completely heterogeneous scenarios whose parameters are those used in Fig. 2. Solid curves correspond, respectively, to (a) Gaussian and (b) Weibull fittings to the data in SIE dynamics. For BP dynamics, the solid curves are fits using typical power laws truncated by a stretched exponential (c)–(e). The parameters used to fit these distributions and statistical metrics are listed in Tables 1 and 2 in the Supplemental Material.

and star graphs in the network. This feature is consistent with the typical network structures seen in the Fig. 4(a) plot. In contrast, at strong allelopathy [see Fig. 4(b)], the average centrality fluctuates probably due to the emergence of modules in the network, as suggested by the typical structures for $\Phi^{(1)}$ and $\mu = 0.5$. In addition, the small values for $\langle x_i \rangle$ are a consequence of very small and sparsely connected network structures. Conversely, for BP, $\langle x_i \rangle$ decreases dramatically as the strength of allelopathic suppression increases. Indeed, even at weak suppression ($\mu = 0.1$, upper plot), strong responses to toxins ($\Phi^{(2)}$) lead to small average centrality. However, in contrast to the SIE dynamics for which a constant $\langle x_i \rangle$ is observed, the centrality is higher for the first species introduced in the community and monotonously decreases for those species attached later.

To further characterize these BP networks, the clustering coefficient and the average degree among nearest neighbors of a node with degree k were also determined. Figure 5(a) shows the average local clustering as a function of in-and out-degree. Our results reveal that both $Cc(k^{\text{in}})$ and $Cc(k^{\text{out}})$ increase slowly for small degrees but exhibit stretched exponential cutoffs for large degrees, i.e., $Cc \sim k^{-\alpha} \exp(-\eta k^{\lambda})$ and $\eta > 0$. The stretched exponential decays of both Cc^{in} and Cc^{out} for large degrees are faster than power-lay decays, $Cc(k) \sim k^{-\alpha}$

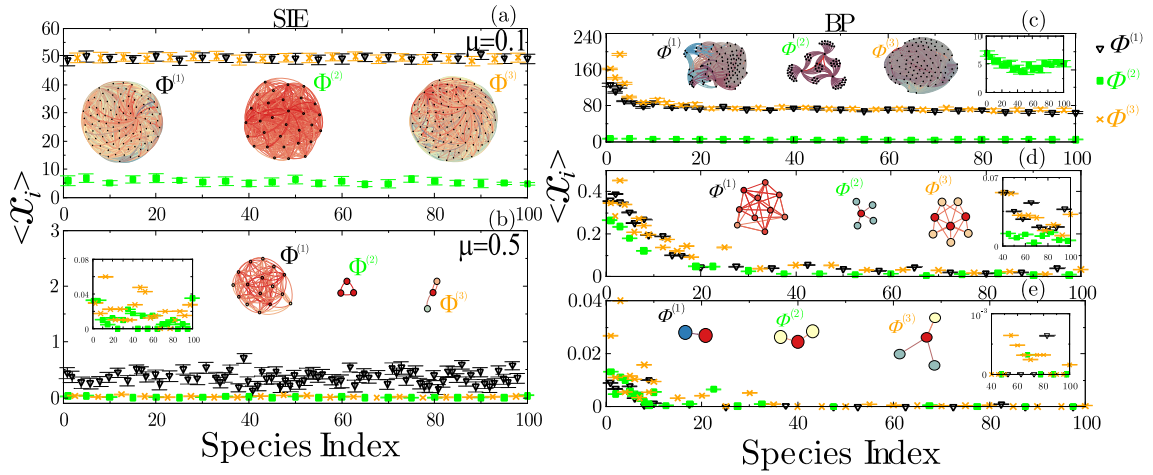

FIG. 4. Average betweenness centrality for each node (surviving species) in communities generated from a single initial species through SIE (a), (b) and from the initial graphs shown in Fig. 1 through the BP dynamics (c)–(e). Typical network structures associated to each functional response are also included. Plots (a) and (b) describe the homogeneous competition and allelopathy at weak ($\mu = 0.1$) and strong ($\mu = 0.5$) allelopathic suppression. Inset: Very small but nonvanishing centralities for the response functions $\Phi^{(2)}$ and $\Phi^{(3)}$ at strong $\mu = 0.5$ allelopathic suppression. Frames (c)–(e) describe, respectively, (c) homogeneous, (d) competition heterogeneous, (e) completely heterogeneous scenarios. Insets: Zooms for small $\langle x_i \rangle$ values. The model parameters are those used in Fig. 3.

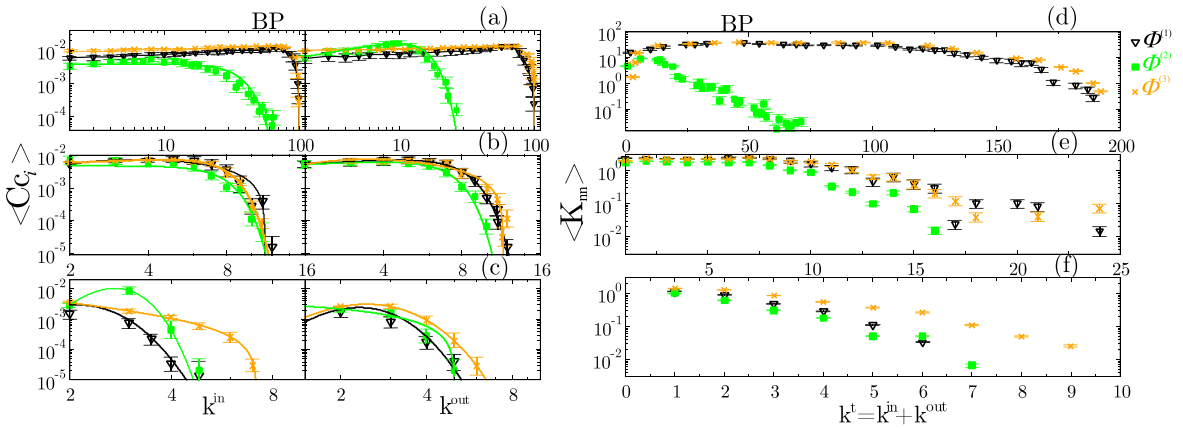

FIG. 5. (a)–(c) Average local clustering coefficient $\langle Cc_i \rangle$ as a function of in and out degrees and average nearest-neighbors degree $\langle K_{nn} \rangle$ of a node with total degree k^t. In both cases, the upper, middle, and bottom plots correspond to the homogeneous, heterogeneous competition, and completely heterogeneous scenarios. The initial networks were all the graphs shown in Fig. 1 and the model parameters are those used in Fig. 3. Specifically, a typical power law truncated by a stretched exponential (solid curve) is fitted to the data of the clustering coefficient (see Table 3 in the Supplemental Material).

with $\alpha \sim 1$, characteristic of modular structures with hierarchical organization [28]. Also, for homogeneous and weak competition and allelopathy, the average clustering coefficient has the same magnitude as those for random networks with the same n, $\langle k^2 \rangle$ and $\langle k \rangle$. However, heterogeneity in competition or strong allelopathic suppression leads to an average clustering coefficient smaller than those for random networks. Since the behavior of Cc is associated to the dynamical mechanisms controlling which new attached node survives or extinguishes, this result indicates that allelochemical networks grow primarily by adding nodes with few links. In Fig. 5(b), we see that K_{nn} decays for the large node's degree even at weak homogeneous allelopathy in a clear disassortative behavior. Such a result is consistent with the observation that assortative mixing by degree makes a network more unstable [29].

Lastly, typical allelochemical networks or community structures generated by the SIE and BP dynamics are illustrated in Figs. 6(a)–6(d) and 6(e)–6(h), respectively. The nodes in these networks represent species present in the community and the directed edges between them represent allelopathic interactions. For the SIE dynamics, as the allelopathic strength increases, the number of nodes (surviving species) decreases, the network topology seems to change from random to modular structures, and the corresponding connectivity distributions change from normal (or Gaussian) to Weibull distributions. In contrast, for the BP dynamics, at weak allelopathic suppression ($\mu = 0.1$), Figs. 6(e) and 6(f), the hierarchical and modular character of such networks emerges. This trait seems to be reflected on the larger values of $\langle x_i \rangle$ for small k, but smaller and almost constant for large k. In turn, for heterogeneous competition and allelopathy, Figs. 6(g) and 6(h), the networks are very small and sparsely connected.

As can be observed, we determined the statistical properties of chemical networks generated after 100 SIE or BP events. As shown in Supplemental Fig. 4, the number of species coexisting at this stage is not so far way from the asymptotic diversity stationary states. However, a relevant issue concerns the dependence of the chemical network's statistical properties on the number of invasion or speciation events. In Supplemental Figs. 7–10, the statistical metrics at the diversity maximum in Fig. 2 were determined. The obtained results were qualitatively the same as those for $n_{SIE} = n_{BP} = 100$, except for SIE average betweenness centrality. As shown in Supplemental Fig. 8, this quantity is not essentially constant as for $n_{SIE} = 100$, but a decreasing function of the index species. The constant behavior seems to be preserved only for $\Phi^{(1,3)}$ functional response at weak allelopathy [Supplemental Fig. 8(a)].

Additional results concerning statistical and network metrics and for response functions involving only the absorbed toxins are reported in the Supplemental Material. The qualitative behavior response functions taking into account only the uptake toxins are the same aforementioned.

IV. DISCUSSION

We have proposed and studied, through numerical methods, an ecoevolutionary model for community assembly involving two coupled processes. The first is a fast ecological dynamic in which species compete for common resources and suppress each other allelopathically. The second are slow evolutionary events in which new species are added to the biological community at its ecological stationary state. Clearly, our study address a basic question: the relation between stability and complexity in the ecology of many interacting species.

All the results obtained here must be analyzed, bearing in mind the scenario for pure intra- and interspecific competition. In the coexistence regime and homogeneous competition ($\nu_{ij} = \nu < 1 \; \forall i, j$), diversity increases linearly with the number l of introduced species, but all their stationary densities, which are inversely proportional to l, vanish as $l \to \infty$. Fully connected communities with high diversity are the rule. In turn, weak ($\nu_{ij} < 1 \; \forall i, j$) and disordered competition can lead several of the introduced and/or resident species to extinction. Therefore, the community diversity tends to be smaller than the number of invasion or speciation events. Yet, all the surviving species at every stationary state constitute fully

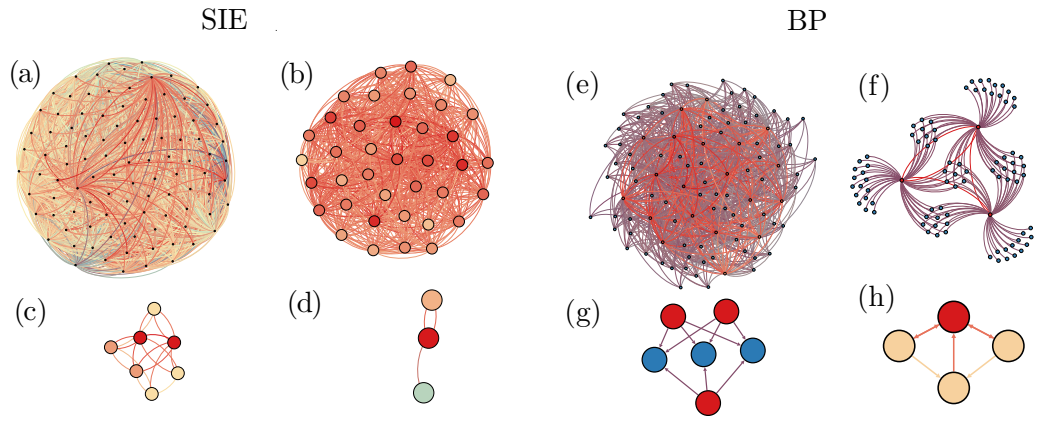

FIG. 6. Typical allelochemical networks generated after $l = 100$ SIEs (a)–(d) and BP (e)–(h). The graphs resulting in the SIE were obtained for (a) weak ($\mu = 0.1$) and (b) strong allelopathic suppression ($\mu = 0.5$) for homogeneous competition and allelochemical traits ($r = 1$, $\nu_{ij} = \gamma_{ij} = 0.1$, $\beta_i = c_i = 0.1$, and $\delta_i = 0.2$ $\forall i, j$). (c) Heterogeneous competition ($\nu_{ij} \in (0, 1]$ randomly chosen, $r = 1$), but weak and homogeneous allelopathy ($\mu_{ij} = \gamma_{ij} = 0.1$, $\beta_i = c_i = 0.1$, $\delta_i = 0.2$ $\forall i, j$). (d) Both competition and allelopathy heterogeneous ($\nu_{i,j}$, $\mu_{i,j}$, β_i, $c_i \in (0, 1]$ randomly chosen, $r = 1$ and $\delta_i = 0.2$). The functional response $\Phi^{(1)}$ was used. For BP generated by speciations, the graph results in a homogeneous scenario ($\nu_{ij} = \gamma_{ij} = 0.1$, $c_i = \beta_i = 0.1$ and $\delta_i = 0.2$ $\forall i, j$) at (a) weak ($\mu = 0.1$) and strong ($\mu = 0.1$) allelopathy. (e) Heterogeneous competition scenario [the same parameters of (d) but randomly chosen competition coefficients ν_{ij}] and (f) completely heterogeneous scenario ($r_i = 1$, $\delta_i = 0.2$ and all other parameters randomly chosen). The starting community structures are those shown in Fig. 1. The response functions $\Phi^{(1)}$ (e) and (f), $\Phi^{(2)}$ (g), and $\Phi^{(3)}$ (h) were used.

connected competition networks, as assumed in our models. This scenario changes considerably in the presence of inhibitory species-species interactions mediated by toxins.

In the SIE dynamics, ecological networks grow through a succession of species immigration. These alien species allelochemically suppress and are suppressed by resident species at random, eventually leading to the eradication of either the invader or some resident species. Our results, shown in Figs. 2(a)–2(c) and Supplemental Fig. 1, reveal that communities exhibiting large diversities can be assembled at weak allelopathy, but diversities are drastically reduced at strong allelopathy for all response functions. In the weak allelopathic regime, the diversity either increases linearly or saturates, depending on response function [see Fig. 2(a)]. For the response functions $\Phi^{(1,3)}$, competition overcomes toxin-mediated suppressions. The reason is that all stationary species densities decrease after each invasion event, consequently reducing the toxin concentrations to very low levels ($B \sim 0$ and $B < c$) for which the response functions are small. This is the reason why we do not expect the community diversity saturation, even for more than $n_{\rm SIE} > 100$. In contrast, for the functional form $\Phi^{(2)}$, the strength of the response to toxins is stronger for very small concentrations in comparison to $\Phi^{(1,3)}$ ($\mathrm{d}\,\Phi^{(i)}(0)/\mathrm{d}B = 1, 1/c, 0$ for, respectively, $i = 1, 2, 3$ and $c < 1$). In this case, diversity saturation is expected because the chemical warfare is enhanced with the introduction of new species. So, the initial increase in diversity for all response functions occurs until a certain number of new introduced species causes a significant allelopathic suppression.

Furthermore, in the strong suppression regime, species richness either saturates or decreases slowly after reaching a maximum. The maxima occur after $\sim 10 - 30$ invasion events, depending on the response function to toxins. At the maxima, the average number of species in the communities never exceeds $16 - 18$ [17]. So, the system of interacting species becomes unstable and the networks stop to grow, consistent with the limit found by May [30]. Beyond these upper bounds, the number of surviving species decreases continuously after each SIE until rest only one (a successful invasion) or very few species. For BP dynamics [see Figs. 2(d)–2(f)], diversity seems to saturate independently on either response functions or allelopathic strength μ. Indeed, every introduced species has suppressive interactions highly correlated to those of its ancestor, in contrast to the random choice of targets in the SIE dynamics. Thus, the chemical warfare is enhanced after each speciation event against a particular subset of target species. Accordingly, network topologies evolve toward marked hierarchical structures, as seen in Figs. 6(a)–6(d), and the corresponding connectivity distributions change from normal (or Gaussian) to Weibull distributions [Figs. 3(a)–3(b)]. Moreover, almost constant average centralities indicate homogeneous connectivity patterns for every node and the absence of hubs, bridges joining distinct modules, and star graphs in the network generated at weak allelopathic suppression. In contrast, at strong allelopathy, networks are very small and sparsely connected, leading to small centrality values [see Figs. 4(a) and 4(b)]. Maybe fluctuations in the small average centralities for strong allelopathic suppression suggest the emergence of modules in the network. Regardless of the regime, such networks comprise a subset of almost null measure in a random ensemble which can only be generated through a constrained growth process.

A major feature in Fig. 2 is that diversity usually reaches a maximum. Then, every new SIE or BP event increases diversity before this maximum but decreases it after the maximum. As suggested by Supplemental Fig. 5, we hypothesize that initially the introduction of new species promotes a relatively uniform increase of node degrees up to a maximally connected network. In this maximally connected network, every node attains its upper degree, which depends on the allelopathy

strength μ and functional response Φ. To overcome this diversity maximum, a further introduction of species tends to induce the extinction of previous species, all of them highly connected and, therefore, strongly threatened. Then, successive SIE or BP events progressively extinct the surviving highly connected species and ultimately generate a stationary network characterized by small numbers of nodes (low diversity) and links (chemical interactions) between them.

The fundamental distinction between the SIE and BP dynamics is that new species are attached to the community with either random or correlated connectivity patterns in the former and the latter case, respectively. Accordingly, species diversity and centrality for BP communities are greater than those for SIE networks (see Figs. 2 and 4). Indeed, each attached species in BP dynamics has, due to its connectivity pattern strongly correlated to that of its ancestor, a smaller chance to destabilize the network. Also, this is the reason why the founders or first species in BP communities have large centrality values in comparison to those almost constant for SIE dynamics (Fig. 4). Additionally, these connectivity correlations foster the emergence of hierarchical and modular structures in BP community networks, as seen in Figs. 6(e)–6(h). These networks have a clear disassortative behavior even at weak homogeneous allelopathy, since the average nearest-neighbors degree $K_{\rm nn}$ decays for the large node's degree [Figs. 5(d)–5(f)]. Such a result is consistent with the observation that assortative mixing by degree makes a network more unstable. Accordingly, the local clustering coefficients for nodes with high degrees k are very small [Figs. 5(a)–5(c)], indicating that species which interact strongly should do so with a few ones, a corollary of May's stability criterium for multispecies communities [30]. Here, the growth process favors the attachment of nodes with few links, since they modify the interaction matrix stability much less than new nodes with many links.

Concerning the main ecological question on the complexity-stability relationship, our findings reveal that high species diversities and dynamical stability of growing ecological networks are very constrained under a widespread biochemical warfare between the interacting species. Indeed, the rate in which species abundance decreases as the number of strong allelopathic interactions increases is faster than those predicted by May's classical analysis [30]. In addition, even in a regime of weak allelopathy, the complexity and stability of ecological networks is drastically impaired by fluctuations in species growth rates exceeding a given threshold. In our simulations, we tested $r_i = r_0\,(1 + \omega_i)$ with ω_i randomly chosen in the range $[-\theta, \theta]$. We observed that extinction begins and, consequently, diversity decreases for $\theta_c > 0.5$. Also, at strong allelopathy, the emerging community networks exhibit average connectivity, degree distributions, and clustering coefficients described by stretched exponentials tails. The clear disassortative behavior of the interaction networks, observed even at weak homogeneous allelopathy generates strongly hierarchical and modular community structures. In contrast, Perotti *et al.* [31], analyzing a model in which new attached nodes to an existing community have interaction coefficients randomly chosen, both positive and negative, found a power-law scaling for such network metrics (connectivity, degree distribution, and clustering coefficient). So, interspecific positive interactions are essential to enhance species persistence, diversity, and community stability. This intuitive expectation was recently demonstrated by Pascual-García and Bastolla [13] who pointed out that mutualism can lead to highly connected and diverse networks when the direct interspecific competition is weaker than a critical value.

Considering our results, the species coexistence in unstructured environments remains unexplained unless the negative allelopathic interactions are weak. A possible alternative to enable the long-term coexistence of complex communities was proposed by Kelsic *et al.* [32]. Analyzing a theoretical model for microbial communities, these authors showed that the combined effect of antibiotic production and degradation can sustain biodiversity. Coexistence depends on the presence of an antibiotic-degrading species which attenuates the inhibitory interactions between two other species. At least two antibiotics are required for stability, but more complex communities and dynamical behaviors emerge for greater numbers of antibiotics. Accordingly, Cordero and Davis [33,6] revealed that environmental bacteria are organized into socially cohesive units in which antagonism occurs between rather than within ecologically defined populations. Within populations, few species produce broad-range antibiotics, whereas all others are resistant, suggesting cooperation between conspecifics.

Summarizing, our major result is that, in allelochemical networks generated either by SIE or BP dynamics, species with strong and negative (inhibitory) interactions are part of systems with a small number of species. Moreover, the interactions tend to be arranged in modules or hierarchies with low clustering coefficients, dissortative behavior and homogeneous and/or heterogeneous degree distributions to ensure community stability. So, communities sustaining large diversities in a homogeneous environment can be assembled only under weak allelopathy. Also, even in this regime the rule is that species interact with a few others. Therefore, in a context of generalized strong allelochemical suppression between organisms, the plankton paradox stands. However, it seems unlikely that biological communities exist under a total biochemical warfare. Thus, for instance, regardless of additional interactions at the level of resource competition, metabolic cross feeding, predator-prey relationships, etc., supposedly there are relevant antagonist relationships between the released allelochemicals. Our model disregards this possibility which promotes alliances between species involved in biochemical warfare. We hypothesize that the coexistence of positive (or activatory) and negative (or inhibitory) interactions is necessary to generate stability and diversity in homogeneous, unstructured environments. Currently, we are focusing on this question.

ACKNOWLEDGMENTS

This work was partially supported by the Brazilian Agencies CAPES (Carvalho graduate fellowship, Finance Code 001), CNPq (306024/2013-6 and 400412/2014-4), and FAPEMIG (APQ-04232-10 and APQ-02710-14).

[1] P. Chesson, Ann. Rev. Ecology Syst. **31**, 343 (2000).
[2] D. Tilman, Princeton University Press **17**, MPB (1982).
[3] G. E. Hutchinson, Am. Nat. **95**, 137 (1961).
[4] D. E. Goldberg and A. M. Barton, Am. Naturalist **139**, 771 (1992).
[5] T. E. Miller, J. H. Burns, P. Munguia, E. L. Walters, J. M. Kneitel, P. M. Richards, N. Mouquet, and H. L. Buckley, Am. Naturalist **165**, 439 (2005).
[6] M. A. Davis, K. J. Wrage, and P. B. Reich, J. Ecol. **86**, 652 (1998).
[7] W. T. Starmer, P. F. Ganter, V. Aberdeen, M.-A. Lachance, and H. J. Phaff, Canadian J. Microbiol. **33**, 783 (1987).
[8] J. Bćahdy, Adv. Appl. Microbiology, 18, 309 (1974).
[9] R. A. Gatenby, E. T. Gawlinski, A. F. Gmitro, B. Kaylor, and R. J. Gillies, Cancer Res. **66**, 5216 (2006).
[10] E. Braganhol, M. R. Wink, G. Lenz, and A. M. O. Battastini, Adv. Exp. Med. Biol. **986**, 81 (2012).
[11] H. P. Bais, S. W. Park, T. L. Weir, R. M. Callaway, and J. M. Vivanco, Trends Plant Sci. **9**, 26 (2004).
[12] R. W. Brooker, F. T. Maestre, R. M. Callaway, C. L. Lortie, L. A. Cavieres, G. Kunstler *et al.*, J. Ecol. **96**, 703 (2008).
[13] A. Pascual-García and U. Bastolla, Nat. Commun. **8**, 14326 (2017).
[14] J. F. Carrion, M. Gastauer, N. M. Mota, and J. A. A. Meira-Neto, J. Arid Env. **142**, 50 (2012).
[15] H. P. Bais, T. S. Walker, F. R. Stermitz, R. A. Hufbauer, and J. M. Vivanco, Plant Physiol. **128**, 1173 (2002).
[16] A. C. Fassoni and M. L. Martins, Ecological Complexity **18**, 49 (2013).
[17] R. Morton and R. Law, J. Theor. Biol. **187**, 321 (1997).
[18] K. Shea and P. Chesson, Trends in Ecology & Evolution **17**, 170 (2002).
[19] N. D. Martinez, Am. Nat. **139**, 1208 (1992).
[20] A. C. Fassoni and M. L. Martins, Ecol. Comp. **18**, 4958 (2014).
[21] S. A. Carvalho and M. L. Martins, Phys. Rev. E **97**, 042403 (2018).
[22] S. A. Carvalho and M. L. Martins, in *Co-Evolution of Secondary Metabolites*, edited by J. Mérillon and K. Ramawat (Springer, Cham, 2020).
[23] A. L. Barabási, *Network science* (Cambridge University Press, Cambridge, 2016), pp. 1–475.
[24] N. Boccara, *Graduate Texts in Physics* (Springer, New York, 2010).
[25] M. E. J. Newman, J. Math. Soc. **37**, 720 (2010).
[26] K. F. Edwards, C. T. Kremer, E. T. Miller, M. M. Osmond, E. Litchman, and C. A. Klausmeier, Ecology Lett. **21**, 1853 (2018).
[27] See Supplemental Material at http://link.aps.org/supplemental/10.1103/PhysRevE.102.042305 for additional information of the model, plots and numerical data of topological properties for different values of the model parameters.
[28] E. Ravasz and A.-L. Barabási, Phys. Rev. E **67**, 026112 (2003).
[29] M. Brede and S. Sinha, arXiv:cond-mat/0507710.
[30] R. M. May, Nature **238**, 413 (1972).
[31] J. I. Perotti, O. V. Billoni, F. A. Tamarit, D. R. Chialvo, and S. A. Cannas, Phys. Rev. Lett. **103**, 108701 (2009).
[32] E. D. Kelsic, J. Zhao, K. Vetsigian, and R. Kishony, Nature **521**, 516 (2015).
[33] O. X. Cordero, H. Wildschutte, B. Kirkup, l. S. Proeh, L. Ngo, F. Hussain, F. Le Roux, T. Mincer, and M. F. Polz, Sci. **337**, 1228 (2012).